Figure S1

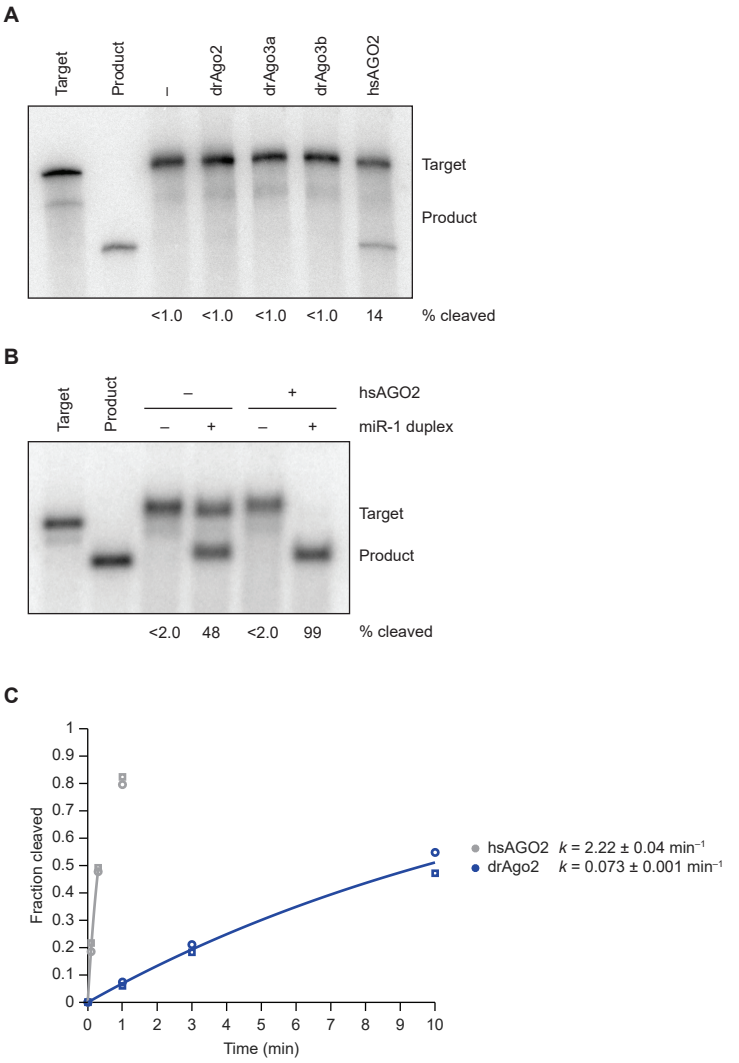

Figure S1. Different Cleavage Efficiencies of drAgo2 and hsAGO2, Related to Figure 1

(A) Activities of the zebrafish Ago paralogs in zebrafish embryos. Assays were as in Figure 1B, injecting mRNA for the indicated proteins. Slicing activity was not observed for drAgo3a and drAgo3b, even though both possess the full catalytic tetrad (DEDH); drAgo1 and drAgo4 were not tested as they had substitutions that disrupted the catalytic tetrad (DEDR and DEGR, respectively).

(B) miR-1–directed slicing in zebrafish embryos. Shown is an RNA blot probing for a miR-1 target co-injected (200 pg/embryo) with or without hsAGO2 mRNA (100 pg/embryo) and with or without exogenous miR-1 duplex (50 fmol/embryo). As previously reported (Giraldez et al., 2005; Cifuentes et al., 2010), slicing catalyzed by endogenous drAgo2 was readily detected. The uncleaved target from the embryo migrated more slowly than the uninjected target, a difference that can be attributed to polyadenylation of the target in the embryo. Likewise, the cleaved product from the embryo migrated more slowly than the standard because it could be generated by cleavage at any of the three miR-1 sites, whereas the standard represented a target cleaved at the 5'-most site.

(C) Plot of slicing time courses resembling those of Figure 1E but using time points more appropriate for fitting rate constants (0.1, 0.3, and 1 min for hsAGO2 and 1, 3, and 10 min for drAgo2). Results for the hsAGO2 and drAgo2 are shown with grey and blue symbols respectively, distinguishing the two replicates (circles, squares). The line for each substrate represents the best fit of the mean values to an exponential reaction course, which generated the rate constants (k, shown ± 95% confidence intervals).

Figure S2

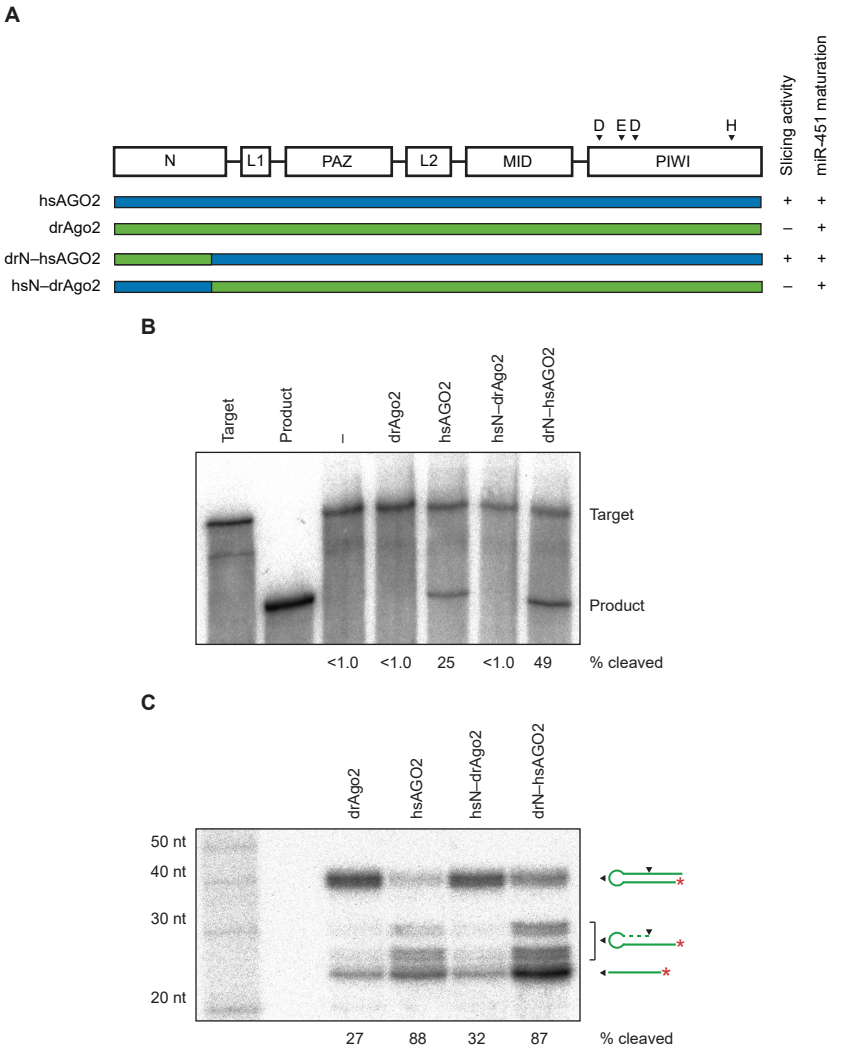

Figure S2. Exploration of Differences in the N Domain as a Source of Reduced Catalytic Activity, Related to Figure 2

(A) Summary of results for a domain-swap experiment, with a schematic representation of the domain and linker architecture of Ago2. Residues of the DEDH catalytic tetrad are indicated above the PIWI domain. Bars show the origin of the respective domains of each parental and chimeric construct, indicating domains from hsAGO2 and drAgo2 in blue and green, respectively. The ability of each construct to slice the miR-430 target in zebrafish embryos or to bind and cleave pre-miR-451 in zebrafish embryos is indicated (+ and –).

(B) Activities of the chimeric constructs, assaying the ability to slice a miR-430 target in zebrafish embryos, as in Figure 1B.

(C) Activities of the chimeric constructs, assaying the ability to bind and cleave pre-miR-451 in zebrafish embryos, as in Figure 3B.

Figure S3

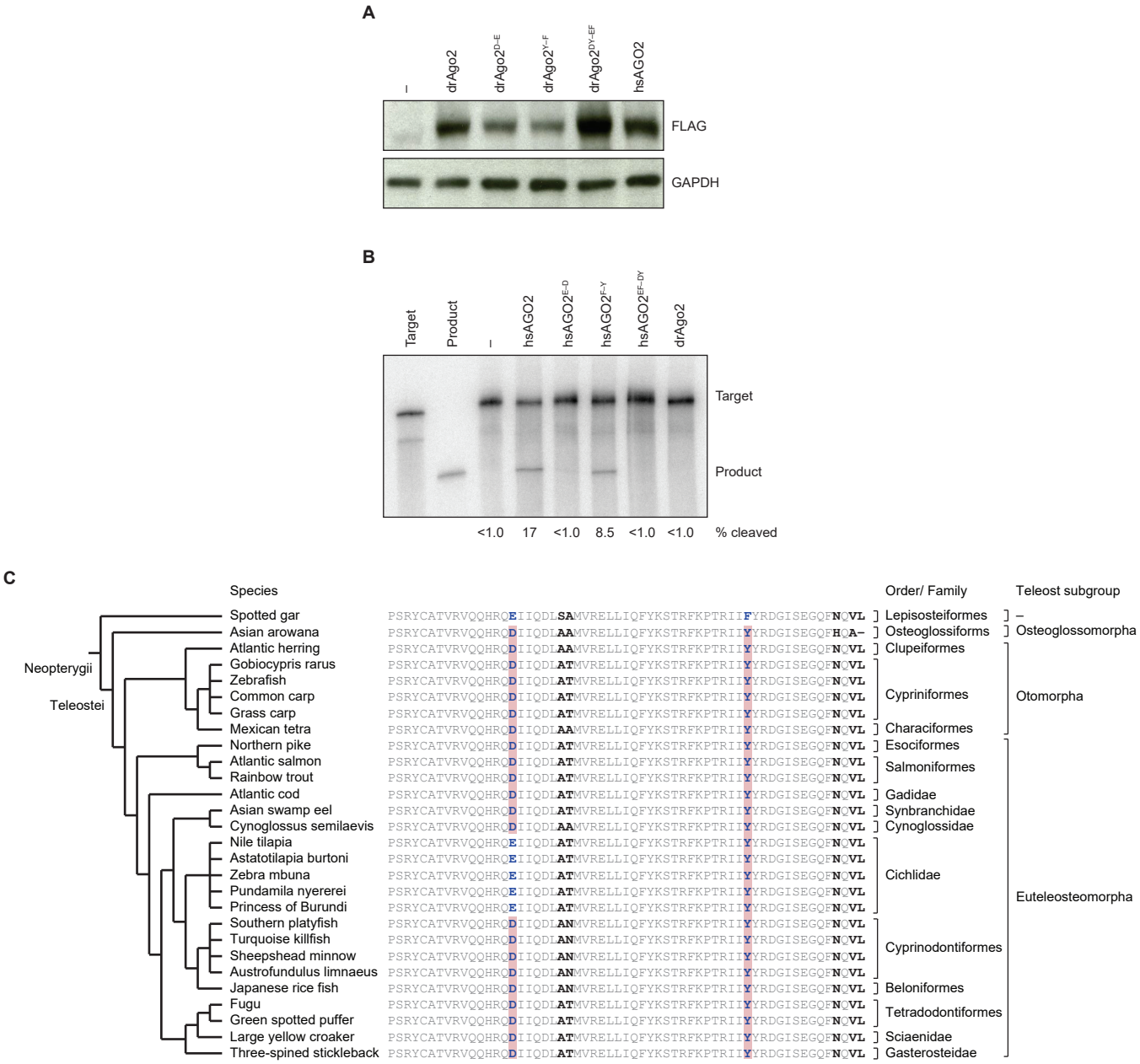

Figure S3. Widespread Presence of Crippling Substitutions Among Teleost Fish, Related to Figure 2

(A) Expression of Ago2 variants in the zebrafish embryo. Shown is an immunoblot probed for FLAG and GAPDH (loading control).

(B) The effects of substituting the zebrafish mutations into the human AGO2 protein, assayed as in Figure 2C.

(C) The inferred origin of the crippling substitutions in an ancestor of the sequenced Teleostei. The cladogram (left) and phylogenetic classification (right) show the evolutionary relationships between all sequenced Teleostei (Bernardi et al., 2012; Betancur et al., 2013). Spotted gar is also shown as an outgroup. The sequence alignment (Tyner et al., 2017) compares a short region of the Ago2 PIWI domain that contains the E-to-D and the F-to-Y substitutions that cripple slicing activity in drAgo2 (shaded in red). Variable residues are in bold. Teleostei fall into four subgroups, the most deeply branching of which (Elopomorpha) had no available sequenced representative. With the exception of the Cichlidae family of Euteleosteomorpha (which has an inferred D-to-E reversion), all sequenced Teleostei possess both of the crippling substitutions.

Figure S4

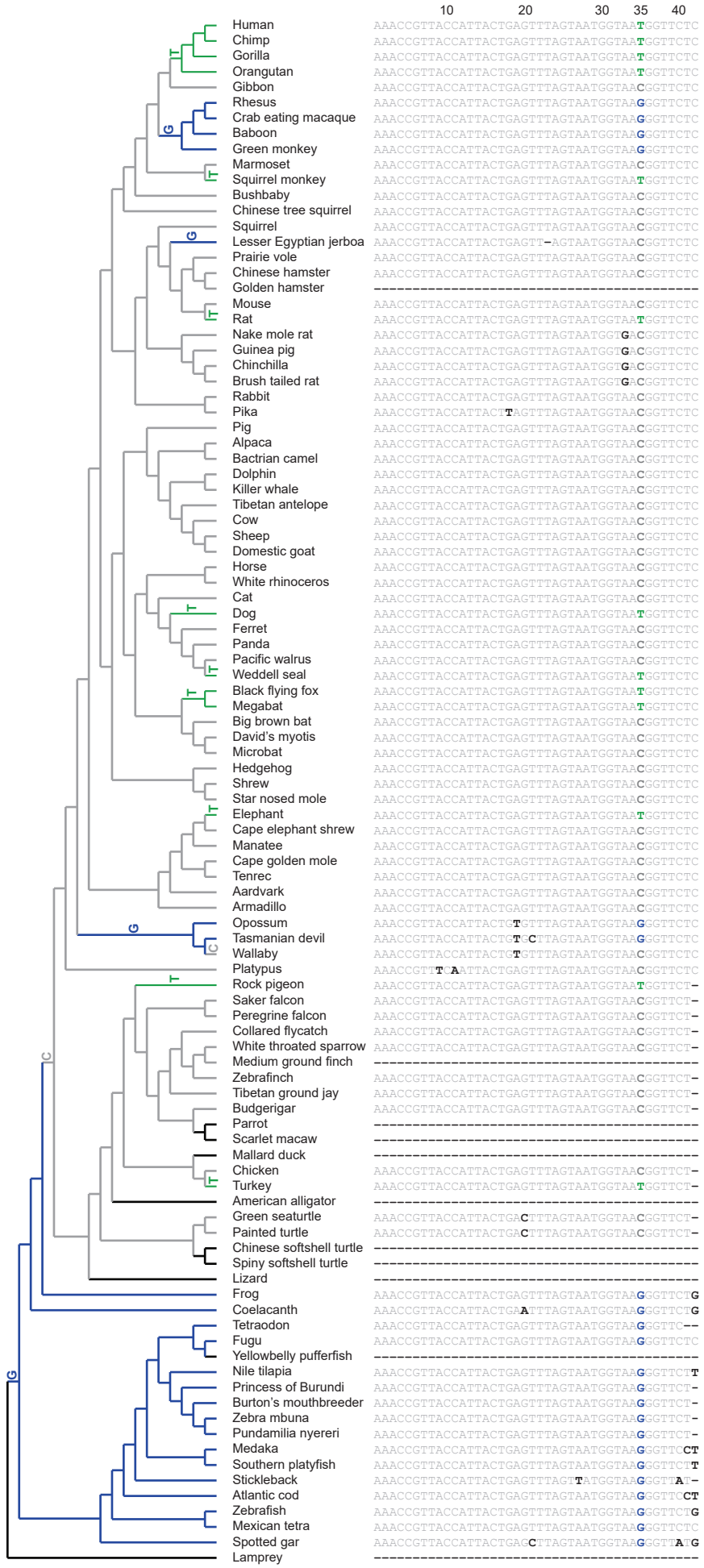

Figure S4. Position 35 of Pre-miR-451 is Highly Variable in Amniotes but Not in Fish, Related to Figure 3

The sequence alignment compares pre-miR-451 DNA sequences from species in the whole-genome alignment (Tyner et al., 2017), highlighting in bold any residues that differ from the inferred ancestral sequence. The residue at position 35 is also highlighted in bold and colored based on its identity (G, blue; C, grey; T, green; not sequenced or not aligned, dashes in alignment and black in cladogram), with the most parsimonious timing and inheritance of substitutions at this position indicated in the cladogram. The ancestral G–G mismatch at positions 6 and 35 is present throughout the fish species, whereas in the amniotes of the whole-genome alignment, the identity of position 35 is variable, with inference of at least 14 events that changed position 35 to C or T, or back to G, as annotated in the cladogram.

Figure S5

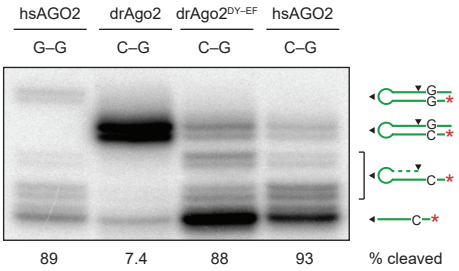

Figure S5. The Effects of a Position-6 C–G Match on Pre-miR-451 Binding and Cleavage, Related to Figure 3

Assays were as in Figure 3E, except lanes 2–4 show the abilities of the zebrafish, repaired zebrafish, and human proteins to bind and cleave pre-miR-451 with a C–G rather than a G–C pair at position 6.

Figure S6

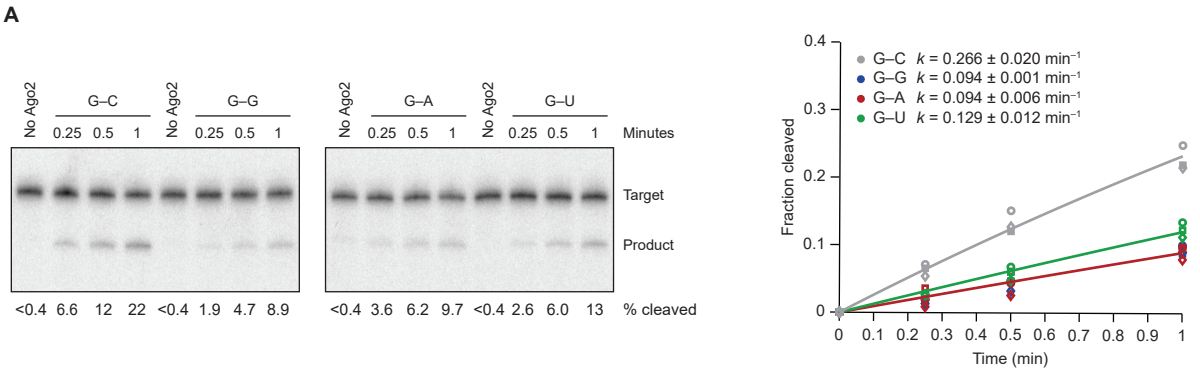

Figure S6. Effects of a G–G Mismatch at guide position 4, Related to Figure 4

The effects of position-4 mismatch on target slicing by miR-430–programmed hsAGO2 in vitro. Otherwise, this panel is as in Figure 4A.

Figure S7

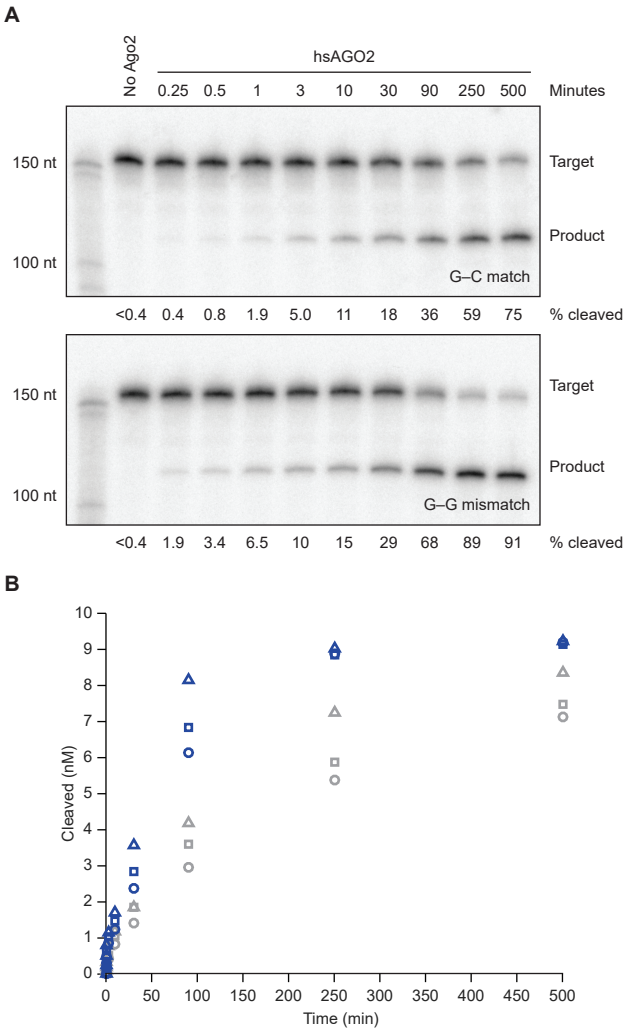

Figure S7. Effects of the G–G Mismatch on Burst and Steady State Kinetics, Related to Figure 5
(A) Raw data for one of the replicates of Figure 5A.
(B) Extension of the Figure 5A plot to include to two later time points taken at 250 and 500 min.

Table S1. Oligonucleotides used in this study, Related to STAR Methods	
DNA	
Name	**Sequence**
Chimera N_for	GCTACTTGTTCTTTTTGCAGGATCC
drAgo2 N_rev	CCTCATGGATGGCAAGTGCCTCATGACAACATCCAGAGCC
hsAGO2 N_rev	CCTCATAGAGGGCAAATGTCTCATGACCACGTCCAGGGCC
drAgo2 body_for	TGGACGGCTACCAAACATCC
hsAGO2 body_for	TGCCTAGCGTCCCTTTTGAG
Chimera body_rev	TGGTTTGTCCAAACTCATCAA
drAgo2 D683A_sense	CATCATCTACTACAGAGCCGGCATCTCTGAAGGCC
drAgo2 D683A_antisense	GGCCTTCAGAGATGCCGGCTCTGTAGTAGATGATG
drAgo2 D651E_sense	CAGCACCGGCAGGAGATCATTCAGGATCTG
drAgo2 D651E_antisense	CAGATCCTGAATGATCTCCTGCCGGTGCTG
drAgo2 Y680F_sense	CCAACACGCATCATCTTCTACAGAGACGGCATC
drAgo2 Y680F_antisense	GATGCCGTCTCTGTAGAAGATGATGCGTGTTGG
hsAGO2 D669A_sense	TCATCTTCTACCGCGCCGGTGTCTCTGAAGG
hsAGO2 D669A_antisense	CCTTCAGAGACACCGGCGCGGTAGAAGATGA
hsAGO2 E637D_sense	GCAGCACCGGCAGGATATCATACAAGACCTG
hsAGO2 E637D_antisense	CAGGTCTTGTATGATATCCTGCCGGTGCTGC
hsAGO2_F666Y_sense	CCCACCCGCATCATCTATTACCGCGACGGTGT
hsAGO2 F666Y_antisense	ACACCGTCGCGGTAATAGATGATGCGGGTGGG
Zeocin target_miR-430_for	ACTGACTCGAGCCTCTAGAAATAAGCTACCCCAACTTGATAGCACTTTATAAGCTATAGTGAGTCGTATTACG
Zeocin target_miR-430_rev	CGTAATACGACTCACTATAGCTTATAAAGTGCTATCAAGTTGGGGTAGCTTATTTCTAGAGGCTCGAGTCAGT
Zeocin_miR-430_10–11 mm_for	ACTGACTCGAGCCTCTAGAAATAAGCTACCCCAACTTCTTAGCACTTTATAAGCTATAGTGAGTCGTATTACG
Zeocin miR-430_10–11 mm_rev	CGTAATACGACTCACTATAGCTTATAAAGTGCTAAGAAGTTGGGGTAGCTTATTTCTAGAGGCTCGAGTCAGT
Zeocin_miR-430_G–G_for	ACTGACTCGAGCCTCTAGAAATAAGCTACCCCAACTTGATAGGACTTTATAAGCTATAGTGAGTCGTATTACG
Zeocin_miR-430_G–G_rev	CGTAATACGACTCACTATAGCTTATAAAGTCCTATCAAGTTGGGGTAGCTTATTTCTAGAGGCTCGAGTCAGT
Zeocin probe_for	ATTCAGGATCATGGCCAAGTTG
Zeocin probe_rev	TTCTAATACGACTCACTATAGGGAGAAGGAGGTTTCTAGAGGCTCGAGTCAGTC
GFP probe	GTCCAGCTCGACCAGGATGGGCACCACCCCGGTGAACAGCTCCTCGCCCTTGCTCACCAT
168-nt target_for	GCGTAATACGACTCACTATAGGGTCACATCTCATCTACCTCC
168-nt target_miR-430_perfect_rev	CCCATTTACATCGCGTTGAGTGTAGAACGGTTGTATAAAAGGTAAAGTGCTATCAAGTTGGGGTAGATCCAGAGGAATTCATTATCAGTG

168-nt target_miR-430_10–11 mm_rev	CCCATTTACATCGCGTTGAGTGTAGAACGGTTGTATAAAAGGTAAAGTGCTAAGAAGTTGGGGTAGATCCAGAGGAATTCATTATCAGTG
168-nt target_miR-430_G–G_rev	CCCATTTACATCGCGTTGAGTGTAGAACGGTTGTATAAAAGGTAAAGTCCTATCAAGTTGGGGTAGATCCAGAGGAATTCATTATCAGTG
168-nt target_miR-430_G–A_rev	CCCATTTACATCGCGTTGAGTGTAGAACGGTTGTATAAAAGGTAAAGTTCTATCAAGTTGGGGTAGATCCAGAGGAATTCATTATCAGTG
168-nt target_miR-430_G–U_rev	CCCATTTACATCGCGTTGAGTGTAGAACGGTTGTATAAAAGGTAAAGTACTATCAAGTTGGGGTAGATCCAGAGGAATTCATTATCAGTG
168-nt target_miR-430_C4_rev	CCCATTTACATCGCGTTGAGTGTAGAACGGTTGTATAAAAGGTAAAGTGCTATCAAGTTGGGGTAGATCCAGAGGAATTCATTATCAGTG
168-nt target_miR-430_G4_rev	CCCATTTACATCGCGTTGAGTGTAGAACGGTTGTATAAAAGGTAAACTGCTATCAAGTTGGGGTAGATCCAGAGGAATTCATTATCAGTG
168-nt target_miR-430_A4_rev	CCCATTTACATCGCGTTGAGTGTAGAACGGTTGTATAAAAGGTAAATTGCTATCAAGTTGGGGTAGATCCAGAGGAATTCATTATCAGTG
168-nt target_miR-430_U4_rev	CCCATTTACATCGCGTTGAGTGTAGAACGGTTGTATAAAAGGTAAAATGCTATCAAGTTGGGGTAGATCCAGAGGAATTCATTATCAGTG
168-nt target_miR-451_C_rev	CCCATTTACATCGCGTTGAGTGTAGAACGGTTGTATAAAAGGTAAACCGTTACCATTACTGAGTTATCCAGAGGAATTCATTATCAGTG
168-nt target_miR-451_G_rev	CCCATTTACATCGCGTTGAGTGTAGAACGGTTGTATAAAAGGTAAACCCTTACCATTACTGAGTTATCCAGAGGAATTCATTATCAGTG
168-nt target_miR-451_A_rev	CCCATTTACATCGCGTTGAGTGTAGAACGGTTGTATAAAAGGTAAACCTTTACCATTACTGAGTTATCCAGAGGAATTCATTATCAGTG
168-nt target_miR-451_U_rev	CCCATTTACATCGCGTTGAGTGTAGAACGGTTGTATAAAAGGTAAACCATTACCATTACTGAGTTATCCAGAGGAATTCATTATCAGTG
168-nt target_miR-1_rev	CCCATTTACATCGCGTTGAGTGTAGAACGGTTGTATAAAAGGTTGGAATGTAAAGAAGTATGTATATCCAGAGGAATTCATTATCAGTG
80-nt target_miR-430	TTGTTGTTGTTGTTGTTGTTAAAGTGCTATCAAGTTGGGGTAGTGTTGTTGTTGTTGTTGTTGTTGTTGCTCCCTATAGTGAGTCGTATTAGAA
80-nt target_miR-430_G–G	TTGTTGTTGTTGTTGTTGTTAAAGTCCTATCAAGTTGGGGTAGTGTTGTTGTTGTTGTTGTTGTTGTTGCTCCCTATAGTGAGTCGTATTAGAA
miR-430 capture	mUmCmUmUmCmCmUmCmCmGmCmAmCmCmAmCmAmCmAmGmCmAmCmUmUmAmAmCmCmUmUmAmCmAmCmAmC/3Bio/
miR-430 competitor	AAGGTTAAGTGCTGTGTGGTGCGGAGGAAGA
miR-451 capture	mUmCmUmUmCmCmUmCmCmGmCmAmCmCmAmCmAmCmAmAmCmGmGmUmUmAmAmCmCmUmUmAmCmAmCmAmC/3Bio/
miR-451 competitor	AAGGTTAACCGTTGTGTGGTGCGGAGGAAGA
miR-1 capture	mUmCmUmUmCmCmUmCmCmGmCmAmCmCmAmCmAmCmAmCmAmUmUmCmCmAmAmCmCmUmUmAmCmAmCmAmC/3Bio/
miR-1 competitor	AAGGTTGGAATGTGTGTGGTGCGGAGGAAGA
RNA	
Name	**Sequence**
miR-430b guide	AAAGUGCUAUCAAGUUGGGGUAG
miR-430b passenger	ACCCUAACUUUAGCAUCUUUCU
pre-miR-451 (ancestral)	AAACCGUUACCAUUACUGAGUUUAGUAAUGGUAAGGGUUCUG
pre-miR-451 (amniote)	AAACCGUUACCAUUACUGAGUUUAGUAAUGGUAACGGUUCUG
miR-1 guide	UGGAAUGUAAAGAAGUAUGUAUdTdT
miR-1 passenger	AUACAUACUUCUUUACAUUCGAdTdT